Effects of Adsorbates on Supported Platinum and Iridium Clusters: Characterization in Reactive Atmospheres and during Alkene Hydrogenation Catalysis by X-ray Absorption Spectroscopy†

Oleg S. Alexeev,‡,§ Fen Li,‡ Michael D. Amiridis,§ and Bruce C. Gates*,‡

Department of Chemical Engineering and Materials Science, University of California, Davis, California 95616, and Department of Chemical Engineering, University of South Carolina, Columbia, South Carolina 29208

Received: March 15, 2004; In Final Form: May 17, 2004

MgO-, SiO_2-, and γ-Al_2O_3-supported platinum clusters and particles (with average diameters ranging from 11 to 45 Å) and zeolite-supported Ir_4 clusters (approximately 6 Å in diameter) were characterized by extended X-ray absorption fine structure spectroscopy in the presence of H_2, O_2, ethene, propene, and ethane, as well as under conditions of alkene hydrogenation catalysis. The results indicate that under various atmospheres, the presence of adsorbates affects the smaller platinum clusters (11 Å) on γ-Al_2O_3 more substantially than the larger platinum particles (i.e., those greater than approximately 21 Å in average diameter) on MgO or SiO_2. When Pt/γ-Al_2O_3 was exposed to H_2, the platinum morphology did not change, although the Pt−Pt bond distance increased. In contrast, when the same sample was exposed to O_2, complete oxidative fragmentation took place. This processes was reversed following subsequent treatment with H_2. Exposure to alkenes changed both the morphology and electron density (as indicated by X-ray absorption near-edge spectra) of the γ-Al_2O_3-supported platinum clusters. Under conditions of alkene hydrogenation catalysis at room temperature, the electronic properties and the structure of the platinum clusters were found to depend on the reactant composition and the nature of molecules involved in the reaction process. The effects of the reactant gases on the smaller iridium clusters (Ir_4) were substantially less pronounced, apparently as a consequence of the extremely small number of atoms in each iridium cluster.

Introduction

Platinum-group metals dispersed on solid supports are important catalysts in many large-scale processes. Years of investigation of these materials have led to a quantitative foundation for understanding the kinetics of reactions on metal surfaces (especially on platinum itself) that is based on measured rates of reactions per exposed metal surface area and recognition of how surface structure affects catalytic activity.[1] This understanding has been developed in part on the basis of recognition of structures that are common to single-crystal surfaces and dispersed particles of the metal. The connection breaks down, however, as the particles become so small that their structures no longer mimic those of bulk crystals and the effects of supports become larger and resemble those of ligands in molecular metal clusters. In the limit—as supported metals become so small that they are clusters of only a few atoms—their properties become distinct and different from those of the bulk; the uniqueness of these clusters offers the prospects of new catalytic properties.

Thus, metal clusters on supports are not generally "metallic"; they may be charged,[2] and—in the presence of reactive mixtures—may undergo structural changes more drastic than those of bulklike metal particles. Such changes may affect the whole cluster and not just the surface, as well as the metal−support interface. To understand how supported metal clusters function as catalysts, it is essential to determine their structures in reactive atmospheres.[3] Extended X-ray absorption fine structure (EXAFS) spectroscopy provides excellent opportunities for structural characterization of supported catalysts in the functioning state. The goal of the research summarized here was to determine how reactive atmospheres influence the structures of supported metal clusters and particles of various sizes. We report EXAFS characterization of MgO-, SiO_2-, and γ-Al_2O_3-supported platinum clusters and particles and zeolite-supported Ir_4 clusters in the presence of O_2, H_2, ethene, propene, and ethane, as well as under conditions of alkene hydrogenation catalysis. Some of these results have been included in a preliminary communication.[4]

Experimental Methods

Reagents and Materials. Powders of γ-Al_2O_3 (Degussa), MgO (EM Science), and SiO_2 (Degussa), with BET surface areas of 100, 47, and 250 m^2/g, respectively, were partially dehydroxylated by treatment in a vacuum at 400 °C. Zeolites NaY and NaX (Grace-Davison) were evacuated at 25 °C for 12 h prior to use. *n*-Pentane solvent was purified by refluxing over Na/benzophenone ketyl and deoxygenated by sparging of N_2. Gases [H_2, N_2, He, ethene, ethane, propene (Matheson, UHP grade)] were purified by passage through traps containing reduced Cu/Al_2O_3 and activated zeolite to remove traces of O_2 and water, respectively. O_2 (Matheson) was purified to remove moisture by passage through a trap containing particles of activated zeolite. The catalyst precursors $PtCl_2(PhCN)_2$ and Ir-$(CO)_2$(acac) (acac is $CH_3COCHCOCH_3$) (each 99% purity, Strem) were used as supplied.

Sample Preparation. Pt/γ-Al_2O_3, Pt/MgO, and Pt/SiO_2 were prepared by slurrying $PtCl_2(PhCN)_2$ with the corresponding

† Part of the special issue "Michel Boudart Festschrift".
‡ University of California.
§ University of South Carolina.

10.1021/jp048907x CCC: $30.25
Published on Web 07/10/2004

TABLE 1: Dispersion of Platinum and of Iridium on Various Supports

sample composition	treatment gas/ temperature (°C)	metal dispersion, fraction of metal sites exposed	average cluster diameter (Å) determined from chemisorption	average cluster diameter (Å) determined from EXAFS	ref
1.0% Pt/γ-Al_2O_3	H_2/400	1.00		11	4
1.0% Pt/MgO	H_2/400	0.54	21	21	4
1.0% Pt/SiO_2	H_2/400	0.25	45		4
1.0% Ir/NaX zeolite	H_2/300	1.00		6.2	this work
1.0% Ir/NaY zeolite	H_2/300	1.00		6.1	this work

powder support in *n*-pentane in amounts chosen to yield samples containing 1 wt % Pt. The pentane was removed by evacuation, ensuring complete uptake of the $PtCl_2(PhCN)_2$ by the support. Prior to characterization, each sample was treated with H_2 at 400 °C to remove organic ligands.

Ir_4/zeolite NaY and Ir_4/zeolite NaX were prepared by a ship-in-a-bottle synthesis technique.[5] In the first step, the precursor $Ir(CO)_2(acac)$ was introduced into the zeolite cages by slurrying with the corresponding zeolite in *n*-pentane for 48 h in amounts appropriate to yield 1 wt % Ir in the catalyst. Then the solvent was removed completely by evacuation and the solid dried under vacuum overnight. Subsequent treatment with CO at 40 or 75 °C for 12 h resulted in the formation of $Ir_4(CO)_{12}$ (ν_{CO}: 2117, 2070, 2060, and 2032 cm^{-1})[6] and $[HIr_4(CO)_{11}]^-$ (ν_{CO}: 2072, 2044, 2035, 2011, and 2000 cm^{-1})[7] in zeolites NaY and NaX, respectively. All the preparation steps and sample transfers were performed with air exclusion techniques by use of Schlenk lines and a N_2-filled glovebox. Prior to the subsequent characterization, each sample was treated with H_2 at 300 °C for 4 h to remove carbonyl ligands. The resultant species were found to incorporate an average of four Ir atoms per cluster.[8,9]

EXAFS Spectroscopy. EXAFS data were collected at X-ray beamlines X-11A and X-18B of the National Synchrotron Light Source (NSLS), Brookhaven National laboratory, Upton, NY. The storage ring energy was 2.5 GeV and the ring current 110−220 mA. Each sample in the powder form was loaded into an in situ EXAFS cell[10] that had been connected to a gas distribution system allowing flow of gases through the sample. The sample mass was chosen to give an absorbance of approximately 2.5 at the Pt L_3 (11563.7 eV) or Ir L_3 (11215 eV) absorption edge, respectively. The EXAFS data were recorded in the transmission mode at room temperature. The data were collected with a Si(111) double-crystal monochromator that was detuned by 20% to minimize the effects of higher harmonics in the X-ray beam.

EXAFS Reference Data and Analysis. The EXAFS data were analyzed with experimentally determined reference files obtained from EXAFS data characterizing materials of known structure, as stated elsewhere.[11] The EXAFS parameters were extracted from the raw data with the aid of the software XDAP.[12] The methods used to extract the EXAFS function from raw data are essentially the same as those reported elsewhere.[13] The data used for each sample were the average of six scans.

The data at the Pt L_3 edge characterizing platinum-containing samples were analyzed with a maximum of 16 free parameters over the ranges of $3.53 < k < 15.69$ $Å^{-1}$ (k is the wave vector) and $0.4 < r < 5.0$ Å (r is the distance from the absorbing atom, in this case Pt). The statistically justified number of free parameters, n, was found to be 36, as estimated on the basis of the Nyquist theorem:[14,15] $n = (2\Delta k \Delta r/\pi) + 1$, where Δk and Δr, respectively, are the k and r ranges used in the data fitting.

The data at the Ir L_3 edge characterizing zeolite-supported samples were analyzed with a maximum of 12 free parameters over the ranges of $3.49 < k < 15.21$ $Å^{-1}$ and $1.0 < r < 3.5$ Å. The statistically justified number of free parameters, estimated as described above, was approximately 20.

The parameters characterizing both the high-Z (Pt−Pt, Ir−Ir) and low-Z (Pt−O and Ir−O) contributions were determined by multiple-shell fitting in both r and k space with application of k^1 and k^3 weighting in the Fourier transformations.[13] The fit was optimized by use of a difference file technique with phase- and amplitude-corrected Fourier transforms of the data.[16,17] The estimated accuracies in determination of EXAFS parameters of the main contributions are as follows: coordination number (N), ±20%; distance (R), ±1%; Debye−Waller factor ($\Delta\sigma^2$), ±30%; inner potential correction (ΔE_0), ±10%.

XANES Measurements and Analysis. X-ray absorption near-edge spectra (XANES) of each sample were obtained in the X-ray absorption experiments. Normalized XANES spectra were obtained by subtracting the preedge background from the raw data with a modified Victoreen equation and dividing the absorption intensity by the height of the absorption edge. The band structure curves were numerically integrated by using the EXAFS data analysis software. The white line area is related to the probability of the transition of 2p electrons to the d states and is correlated with the electron density on metal atoms. An increase in the white line area indicates a decrease in the electron density on metal atoms.

Results

Metal Dispersions. The average platinum cluster size and dispersion were estimated on the basis of hydrogen chemisorption data and EXAFS data, the latter interpreted on the basis of the model reported by Kip et al.[18] relating the average cluster size to the metal−metal first-shell coordination number. The data (Table 1) indicate that platinum clusters with an average diameter of about 11 Å were formed on the γ-Al_2O_3 support following exposure of the sample to H_2 at 400 °C. Assuming spherical clusters, this size corresponds to a metal dispersion of essentially 100% and indicates that each cluster incorporates on average approximately 25 atoms. Similar treatment of Pt/MgO and Pt/SiO_2 led to the formation of larger clusters (particles), with average diameters of approximately 21 and 45 Å, respectively. A comparison of the phase- and amplitude-corrected Fourier transforms (k^3 weighted) characterizing the first-shell Pt−Pt contributions in platinum on the various supports is shown in Figure 1.

Upon decarbonylation of $[HIr_4(CO)_{11}]^-$/zeolite NaX and $Ir_4(CO)_{12}$/zeolite NaY in H_2 at 300 °C, the tetrahedral cluster frame remained essentially unchanged (as evidenced by the Ir−Ir coordination numbers of approximately 3). The four-atom clusters have an average diameter of about 6 Å.

Strategy for Elucidation of Effects of Adsorbates on Supported Metals. In attempts to unravel the effects on the catalysts of the various reactants present during catalytic hydrogenation of alkenes, we investigated the influence of each reactant and product individually on the supported catalysts and also the influence of alkene, H_2, and alkane in combination (as catalytic hydrogenation occurred).

Effect of H_2 on Supported Platinum Clusters. Supported platinum samples were characterized by EXAFS spectroscopy,

TABLE 2: EXAFS Results at the Pt L_3 Edge Characterizing the Interaction of H_2 at 25 °C with Supported Pt Samples Pre-Reduced with H_2 at 400 °C[a]

sample	average cluster diameter, Å	conditions during scan	shell	Pt−Pt contributions				Pt−$O_{support}$ (Pt−O_s[b] and Pt−O_l[c]) contributions			
				N	R (Å)	$10^3\Delta\sigma^2$	ΔE_0 (eV)	N	R (Å)	$10^3\Delta\sigma^2$	ΔE_0 (eV)
Pt/γ-Al_2O_3	11	vacuum	first	6.4	2.70	6.77	3.5	0.7[b]	2.12	10.0	0.6
								0.6[c]	2.77	7.84	−6.73
		H_2 flow	first	6.5	2.76	4.87	−0.1	0.3[b]	2.21	10.0	−10.0
								0.5[c]	2.70	10.0	0.0
Pt/MgO	21	vacuum	first	8.7	2.75	2.25	1.4	0.5[b]	2.09	10.0	3.3
			second	5.8	3.89	4.70	−3.5				
			third	11.1	4.78	10.0	−7.0				
		H_2 flow	first	8.6	2.75	2.30	0.0	0.2[b]	2.09	7.1	0.0
			second	5.6	3.88	6.40	1.0				
			third	11.9	4.76	10.0	−5.4				
Pt/SiO_2	45	vacuum	first	11.2	2.76	0.80	−0.9	0.2[b]	2.18	10.0	0.0
			second	6.0	3.90	0.40	0.0				
			third	15.4	4.75	6.50	−4.0				
		H_2 flow	first	11.0	2.76	0.50	−0.7	0.2[b]	2.18	10.0	0.0
			second	6.0	3.88	0.40	4.0				
			third	16.9	4.75	6.60	−3.6				

[a] Notation: N, coordination number; R, distance between absorber and backscatterer atoms; $\Delta\sigma^2$, Debye−Waller factor; ΔE_0, inner potential correction; the subscripts s and l refer to short and long, respectively.

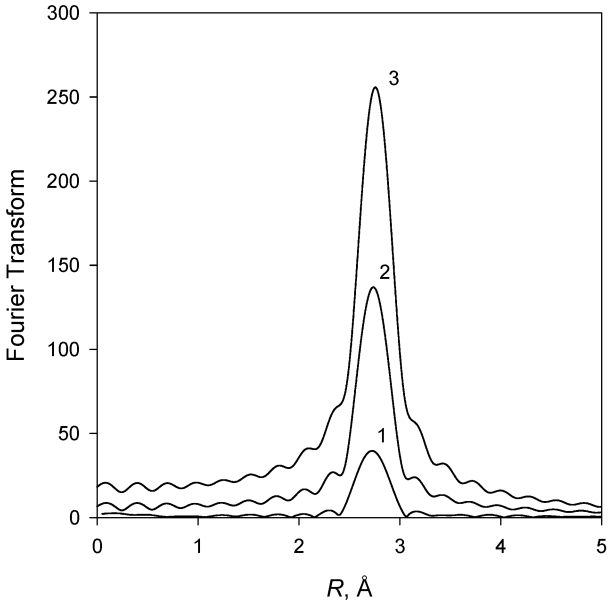

Figure 1. Phase- and amplitude-corrected Fourier transforms (k^3 weighted) characterizing the first-shell Pt−Pt contributions in Pt samples treated with H_2 at 400 °C and exposed to H_2 flow at 25 °C: (1) Pt/γ-Al_2O_3; (2) Pt/MgO; (3) Pt/SiO_2.

both under vacuum and in contact with H_2 at atmospheric pressure. The results (Table 2) show that the γ-Al_2O_3-supported clusters under vacuum are characterized by a first-shell Pt−Pt coordination number of 6.4 at a distance of 2.70 Å. After exposure of the sample to H_2 at 25 °C, the first-shell Pt−Pt coordination number remained essentially unchanged, but the Pt−Pt distance increased to 2.76 Å (Table 2). After subsequent evacuation at 25 °C, the EXAFS data matched those observed initially for Pt/γ-Al_2O_3 under vacuum, showing the reversibility of the changes induced by H_2.

The EXAFS data show further that H_2 affected the metal−support interface. The Pt−O_s contributions (the subscript s refers to short), characterizing the bonding interaction of platinum with the support, were substantially longer with the sample in the presence of H_2 (2.21 Å) than under vacuum (2.12 Å) (Table 2).

In contrast, no detectable changes in the Pt−Pt bond distance were observed when the larger clusters (particles) in Pt/MgO and Pt/SiO_2 were exposed to H_2 (Table 2); the behavior is that expected for bulklike platinum metal.

Effect of O_2 on γ-Al_2O_3-Supported Platinum Clusters. When a completely reduced sample of Pt/γ-Al_2O_3 was exposed to doses of O_2 in N_2 at 25 °C, the value of N_{Pt-Pt} decreased from 6.5 to 4.2 and the value of R_{Pt-Pt} decreased from 2.76 to 2.68 Å, consistent with the partial oxidation of platinum and a decrease of the platinum cluster size. This change was accompanied by an increase of the Debye−Waller factor characterizing the Pt−Pt contributions (Table 3), indicating a higher degree of disorder in the sample after interaction with O_2. Substantial changes were also observed in the metal−support interface. The Pt−O_s coordination number increased and the Pt−O_s distance decreased relative to the values characterizing the unoxidized sample (Table 3), consistent with the larger number of oxygen atoms bonded to the platinum in the partially oxidized sample.

When the sample was treated with more doses of O_2 in N_2 at 25 °C, leading to a higher degree of oxidation of platinum, the EXAFS data gave no indication of remaining Pt−Pt contributions, consistent with a complete conversion of platinum to platinum oxide species. The platinum clusters were evidently completely oxidized.[19]

Effect of H_2 on Completely Oxidized Pt/γ-Al_2O_3. When the bed of particles of sample containing the completely oxidized platinum clusters was exposed at 25 °C to the first portion of H_2 dosed into the N_2 stream flowing continuously through it, the values of N_{Pt-Pt} and R_{Pt-Pt} increased to 2.7 and 2.75 Å, respectively, indicating partial conversion of the oxidized platinum clusters back into platinum clusters (Table 3). Additional dosing of H_2 led to a gradual increase of N_{Pt-Pt} to 6.5, with the value of R_{Pt-Pt} remaining essentially unchanged, consistent with complete conversion of the oxidized platinum clusters into platinum clusters in their original state and the same average size (Table 3).

Effect of Alkenes and Alkanes on Supported Platinum Clusters and Particles of Various Sizes. When completely reduced Pt/γ-Al_2O_3 was exposed to a flow of propene or ethene at atmospheric pressure and 25 °C, the values of N_{Pt-Pt} decreased from 6.5 to 4.1 or 3.0, respectively, and the value of R_{Pt-Pt} became equal to that characterizing the sample under vacuum (2.71 Å) (Tables 2 and 4). The decrease in N_{Pt-Pt} was accompanied by increases in the Debye−Waller factors, and

TABLE 3: EXAFS Results at the Pt L_3 Edge Characterizing the Effects of O_2/H_2 Treatments at 25 °C on the Structure of γ-Al_2O_3-Supported Platinum Clusters[a]

feed composition during scan[b]	first-shell Pt−Pt contributions				Pt−$O_{support}$ (Pt−O_s) contribution				Pt−$O_{support}$ (Pt−O_l) contribution			
	N	R (Å)	$10^3\Delta\sigma^2$	ΔE_0 (eV)	N	R (Å)	$10^3\Delta\sigma^2$	ΔE_0(eV)	N	R (Å)	$10^3\Delta\sigma^2$	ΔE_0 (eV)
H_2 flow	6.5	2.76	4.87	−0.1	0.3	2.21	10.0	−10.0	0.5	2.70	10.0	0.0
O_2 dosing in N_2 flow	4.2	2.68	9.90	−2.2	2.0	2.08	4.9	−1.0	0.1	2.65	−8.0	−2.8
O_2 dosing in N_2 flow	0.0	0.0	0.0	0.0	2.7	2.09	4.6	−2.4	0.7	2.62	−5.6	−6.0
H_2 dosing in N_2 flow	2.7	2.75	1.80	1.0	1.0	2.08	10.0	10.4	1.8	2.61	10.0	5.2
H_2 dosing in N_2 flow	3.0	2.77	1.95	−1.5	0.7	2.15	10.0	−10.0	0.6	2.74	−5.0	−4.1
H_2 dosing in N_2 flow	3.7	2.77	2.00	−2.4	0.7	2.22	10.0	−14.1	0.4	2.72	−7.4	−2.1
H_2 dosing in N_2 flow	4.4	2.77	2.29	−2.1	0.7	2.22	10.0	−14.1	0.4	2.72	−7.4	−1.9
H_2 dosing in N_2 flow	4.8	2.77	2.45	−2.0	0.7	2.22	10.0	−14.1	0.3	2.72	−7.9	−0.8
H_2 dosing in N_2 flow	5.9	2.77	3.00	−1.8	0.8	2.21	10.0	−13.4	0.3	2.72	−7.3	1.0
H_2 dosing in N_2 flow	6.5	2.76	4.87	−0.1	0.6	2.21	10.0	−10.1	0.5	2.70	10.0	0.0

[a] Notation as in Table 2. [b] Experiments were performed in the sequence listed.

TABLE 4: EXAFS Results at the Pt L_3 Edge Characterizing the Interactions of γ-Al_2O_3-Supported Platinum Clusters with Alkenes and Alkanes[a]

feed composition during scan[b]	first-shell Pt−Pt contributions				Pt−$O_{support}$ (Pt−O_s) contribution				Pt−$O_{support}$ (Pt−O_l) contribution			
	N	R (Å)	$10^3\Delta\sigma^2$	ΔE_0 (eV)	N	R (Å)	$10^3\Delta\sigma^2$	ΔE_0 (eV)	N	R (Å)	$10^3\Delta\sigma^2$	ΔE_0 (eV)
H_2 flow	6.5	2.76	4.87	−0.1	0.3	2.21	10.0	−10.0	0.5	2.70	10.0	0.0
C_3H_6 flow	4.1	2.71	5.30	4.8	0.7	2.08	4.1	1.0	0.7	2.63	1.4	−0.8
H_2 flow	6.6	2.76	4.90	−0.1	0.3	2.21	6.9	−13.0	0.2	2.78	−4.3	−2.0
C_2H_4 flow	3.0	2.71	5.50	3.6	1.2	2.14	10.0	−6.7	0.7	2.66	3.9	−1.5
H_2 flow	6.5	2.76	4.70	0.1	0.4	2.22	10.0	−17.3	0.2	2.75	−8.3	5.9
C_2H_6 flow	5.6	2.75	4.20	−0.1	0.5	2.19	10.0	−6.0	0.8	2.72	7.9	−3.0
H_2 flow	6.3	2.77	4.50	−0.2	0.5	2.22	10.0	−16.8	0.4	2.74	−8.4	4.4

[a] Notation as in Table 2. [b] Experiments were performed in the sequence listed.

TABLE 5: EXAFS Results at the Pt L_3 Edge Characterizing the Larger Interaction of Platinum Particles with Alkenes and Alkanes[a]

sample	average Pt particle size (Å)	conditions during scan	shell	Pt−Pt contributions				Pt−$O_{support}$ contribution			
				N	R (Å)	$10^3\Delta\sigma^2$	ΔE_0 (eV)	N	R (Å)	$10^3\Delta\sigma^2$	ΔE_0 (eV)
Pt/MgO	21	H_2 flow	first	8.6	2.75	2.3	0.0	0.2	2.09	7.1	0.0
			second	5.6	3.88	6.4	1.0				
			third	11.9	4.76	10.0	−5.4				
		C_3H_6 flow	first	8.5	2.75	2.2	0.2	0.6	2.09	10.0	2.5
			second	5.5	3.85	4.5	5.5				
			third	10.0	4.74	8.7	−4.8				
		C_2H_4 flow	first	8.5	2.74	3.1	0.7	0.8	2.09	10.0	2.5
			second	2.2	3.86	0.1	4.4				
			third	7.1	4.74	6.9	−4.8				
Pt/SiO_2	45	H_2 flow	first	11.0	2.76	0.5	−0.7	0.2	2.18	10.0	0.0
			second	6.0	3.88	0.4	4.0				
			third	16.9	4.75	6.6	−3.6				
		C_3H_6 flow	first	11.0	2.76	0.5	−0.6	0.2	2.18	10.0	0.0
			second	6.0	3.88	0.0	3.5				
			third	16.5	4.75	6.5	−3.8				
		C_2H_4 flow	first	11.3	2.76	0.8	−0.8				
			second	6.0	3.88	0.2	3.5				
			third	16.9	4.75	6.9	−3.8				

[a] Notation as in Table 2.

the process was reversible, as evidenced by the data obtained upon reexposure of the sample to H_2 at 25 °C (Table 4).

Exposure of the sample to flowing ethane at atmospheric pressure and 25 °C led to much smaller changes in N_{Pt-Pt}, which were directionally the same as those caused by the alkenes (Table 4).

When the larger platinum particles (approximately 21 Å in average diameter) in Pt/MgO were similarly exposed to ethane, no changes in EXAFS parameters were observed (Table 5). Similarly, exposure of this sample to flowing ethene did not lead to substantial changes in the EXAFS parameters characterizing the first Pt−Pt coordination shell. However, the values of N_{Pt-Pt} for the second and the third coordination shells were found to be 2.2 and 7.1, respectively, and these are substantially less than the corresponding values determined for the sample that had been exposed to H_2 (Table 5). The small changes undergone by the intermediate-sized particles in this sample indicate that at a diameter of approximately 21 Å they already exhibit a nearly bulklike behavior. This result was confirmed by results characterizing the Pt/SiO_2, incorporating platinum particles with an average diameter of approximately 45 Å, which were found to be insensitive to the treatment environment (Table 5), indicating that they are clearly bulklike.

EXAFS Data Characterizing Surface Species under Catalytic Reaction Conditions. The relatively small (11 Å) platinum clusters on γ-Al_2O_3 were also characterized by EXAFS spectroscopy during catalytic hydrogenation of ethene and of propene at 25 °C, with the EXAFS cell serving as a flow reactor. The EXAFS data show how the structure of highly dispersed platinum clusters on γ-Al_2O_3 depends on the feed composition

TABLE 6: EXAFS Results at the Pt L_3 Edge Recorded during Alkene Hydrogenation Catalyzed by γ-Al_2O_3-Supported Platinum Clusters at 25 °C [a]

feed composition during scan[b]	effluent gas-phase composition	first-shell Pt−Pt contributions				Pt−$O_{support}$ (Pt−O_s) contribution				Pt−$O_{support}$ (Pt−O_l) contribution			
		N	R (Å)	$10^3\Delta\sigma^2$	ΔE_0 (eV)	N	R (Å)	$10^3\Delta\sigma^2$	ΔE_0 (eV)	N	R (Å)	$10^3\Delta\sigma^2$	ΔE_0 (eV)
C_3H_6/H_2 flow (2:1 ratio)	C_3H_6/C_3H_8 (1:1 ratio)	4.0	2.71	5.3	4.8	0.9	2.14	6.5	−7.5	0.4	2.63	1.4	−0.8
H_2 flow		6.6	2.76	4.9	−0.1	0.3	2.21	6.9	−13.0	0.2	2.78	−4.3	−2.0
C_2H_4/H_2 (5:1 ratio)	C_2H_4/C_2H_6 (4:1 ratio)	3.0	2.70	5.3	3.8	1.2	2.14	9.8	−6.7	0.7	2.66	3.2	−1.5
C_2H_4/H_2 (1:1 ratio)	C_2H_6	5.7	2.75	5.5	0.0	0.5	2.19	10.0	−6.6	0.6	2.74	10.0	−3.4
H_2 flow		6.5	2.76	4.9	0.3	0.5	2.21	10.0	−10.0	0.7	2.70	10.0	−2.5

[a] Notation as in Table 2. [b] Experiments were performed in the sequence as listed.

TABLE 7: EXAFS Results at the Ir L_3 Edge Recorded during Alkene Hydrogenation Catalyzed by Zeolite-Supported Ir_4 Clusters at 25 °C[a]

sample	feed composition during scan[b]	effluent gas-phase composition	first-shell Ir−Ir contributions				Ir−$O_{support}$ (Ir−O_s) contribution				Ir−$O_{support}$ (Ir−O_l) contribution			
			N	R (Å)	$10^3\Delta\sigma^2$	ΔE_0 (eV)	N	R (Å)	$10^3\Delta\sigma^2$	ΔE_0 (eV)	N	R (Å)	$10^3\Delta\sigma^2$	ΔE_0 (eV)
Ir_4/ zeolite NaY	H_2 flow		3.3	2.69	2.6	−0.4	2.2	2.19	0.7	−12.1	1.7	2.61	3.5	−7.7
	C_2H_4 flow	C_2H_4	3.0	2.69	2.3	0.5	2.1	2.18	0.6	−11.1	1.5	2.61	0.5	−6.1
	H_2 flow		3.2	2.70	2.5	−0.5	2.1	2.19	0.6	−12.3	1.3	2.63	0.4	−7.7
	C_2H_4/H_2 (2:1 ratio)	C_2H_4/C_2H_6 (1:1 ratio)	3.0	2.69	2.4	0.2	2.3	2.19	1.1	−12.6	1.7	2.62	3.2	−8.5
	C_2H_4/H_2 (1:1 ratio)	C_2H_6	3.0	2.69	2.5	−0.3	2.2	2.19	0.5	−12.7	1.4	2.63	2.3	−8.6
	H_2 flow		3.2	2.70	2.6	0.3	2.0	2.20	0.3	−12.9	1.4	2.62	1.8	−8.1
Ir_4/ zeolite NaX	H_2 flow		3.1	2.72	1.5	−5.0	0.8	2.11	10.0	−8.3	1.0	2.63	−4.6	1.6
	C_2H_4 flow	C_2H_4	3.0	2.72	2.0	−5.0	1.3	2.12	10.0	−7.9	0.6	2.63	−5.7	2.5
	H_2 flow		3.0	2.72	3.0	−5.0	1.4	2.09	10.0	−4.1	1.0	2.68	−4.7	−5.2
	C_2H_4/H_2 (2:1 ratio)	C_2H_4/C_2H_6 (1:1 ratio)	3.0	2.71	3.5	−2.0	1.8	2.05	10.0	0.4	1.2	2.67	−3.5	−5.4
	C_2H_4/H_2 (1:1 ratio)	C_2H_6	3.0	2.72	2.6	−4.4	1.3	2.10	10.0	−5.6	1.0	2.67	−4.5	−3.9
	H_2 flow		3.0	2.72	2.6	−4.8	1.3	2.13	10.0	−8.2	1.0	2.67	−5.0	−4.9

[a] Notation as in Table 2. [b] Experiments were performed in the sequence as listed.

(Table 6). For example, when the amount of H_2 in the feed was not enough for complete hydrogenation of ethene or propene—so that alkenes were the predominant reactants present in the reactant stream in contact with the catalyst—the values of N_{Pt-Pt} and R_{Pt-Pt} were found to be the same as those observed when only ethene or propene alone flowed through the sample cell (Tables 4 and 6). On the other hand, when the amount of H_2 in the feed was enough for complete hydrogenation of ethene to ethane, the values of N_{Pt-Pt} and the R_{Pt-Pt} were found to be 5.7 and 2.75 Å, respectively, which match those observed for the sample exposed to ethane alone. The data summarized in Table 6 demonstrate not only dynamic changes in the morphology of the γ-Al_2O_3-supported platinum clusters, depending on the composition of the reaction mixture, but also the near reversibility of the induced changes: For example, treatment of the sample exposed to reaction conditions with H_2 at 25 °C led to values of N_{Pt-Pt} and R_{Pt-Pt} that are similar to those characterizing the initially reduced sample (Table 4).

Effect of Adsorbates on Supported Iridium Clusters. In contrast to the results characterizing supported platinum clusters, the EXAFS data summarized in Table 7 show that the structural parameters characterizing the zeolite NaY- or NaX-zeolite-encaged Ir_4 clusters remained essentially unchanged under catalytic reaction conditions. When the Ir_4/NaY zeolite sample was subjected to H_2 flow only (the EXAFS data at the Ir L_{III} edge characterizing this sample are shown in Figure 2), the values of N_{Ir-Ir} and R_{Ir-Ir} were 3.3 and 2.69 Å, respectively. When the sample was subjected to the flow of ethane only (Figure 3), the values of N_{Ir-Ir} and R_{Ir-Ir} were found to be 3.0 and 2.69 Å, respectively. When further treatment was carried out either in H_2 or a mixture of H_2 and ethene (no matter which was present in excess), the maximum changes of the values of N_{Ir-Ir} and R_{Ir-Ir} were only 0.3 and 0.02 Å, respectively. These differences are within the estimated experimental error. Similar results were also obtained with the Ir_4/NaX zeolite sample; again, the changes were within the experimental error (0.1 for N_{Ir-Ir}, and 0.01 Å for R_{Ir-Ir}).

XANES Results. The XANES regions of the spectra were analyzed to provide further evidence of the influence of H_2, O_2, alkenes, and alkanes on the electronic structures of the supported platinum clusters and particles. The results (Table 8) show that when Pt/γ-Al_2O_3 was exposed to O_2, the area under the white line increased substantially (relatively, from 11.8 to 14.5), consistent with the suggestion that platinum in this sample had a lower electron density than that in the reduced sample. After adsorption of ethane on Pt/γ-Al_2O_3, the white line area also increased relative to that of the sample scanned under vacuum (Table 8). Addition of H_2 to the flowing stream of ethene led to changes in the white line area depending on the concentration of H_2 in the feed. When the amount of H_2 was enough to convert all the ethene to ethane, the white-line area was the same as that observed after contacting of the sample with ethane (Table 8).

In contrast, the XANES data characterizing Ir_4/NaX zeolite and Ir_4/NaY zeolite do not show any systematic variations resulting from exposure of the samples to various reactants. The observed variations in these data (Table 8) are within the experimental uncertainties, which may be as high as 10%.[20]

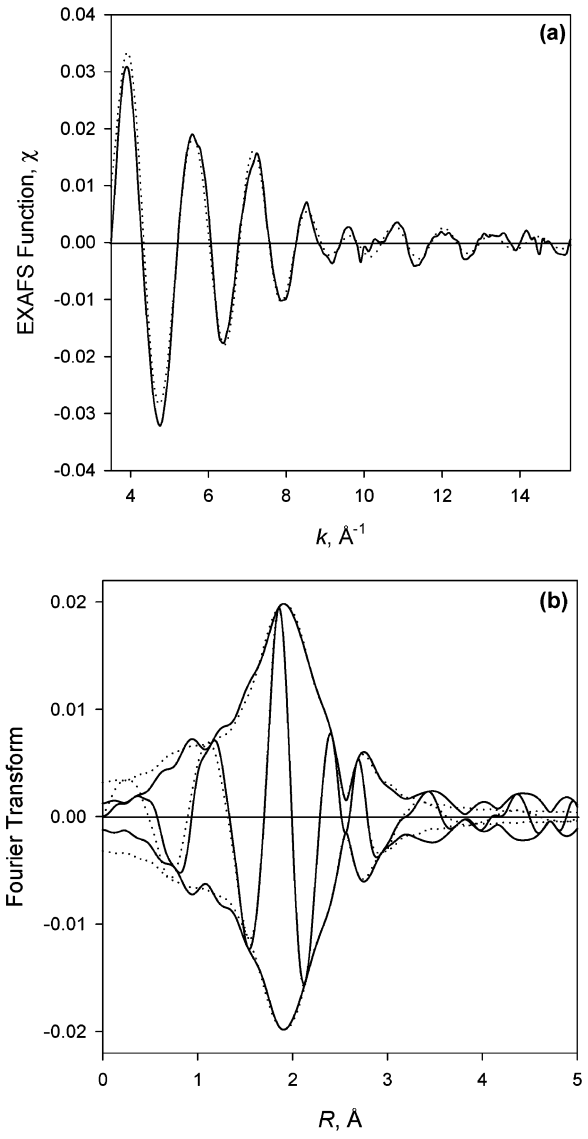

Figure 2. Results of EXAFS analysis characterizing Ir_4/NaY zeolite sample subjected to H_2 flow: (a) experimental EXAFS (χ) function (solid line) and the sum of the calculated contributions (dotted line); (b) imaginary part and magnitude of uncorrected Fourier transform (k^0 weighted, $\Delta k = 3.5-15.3$ Å^{-1}) of experimental EXAFS (solid line) and sum of the calculated contributions (dotted line).

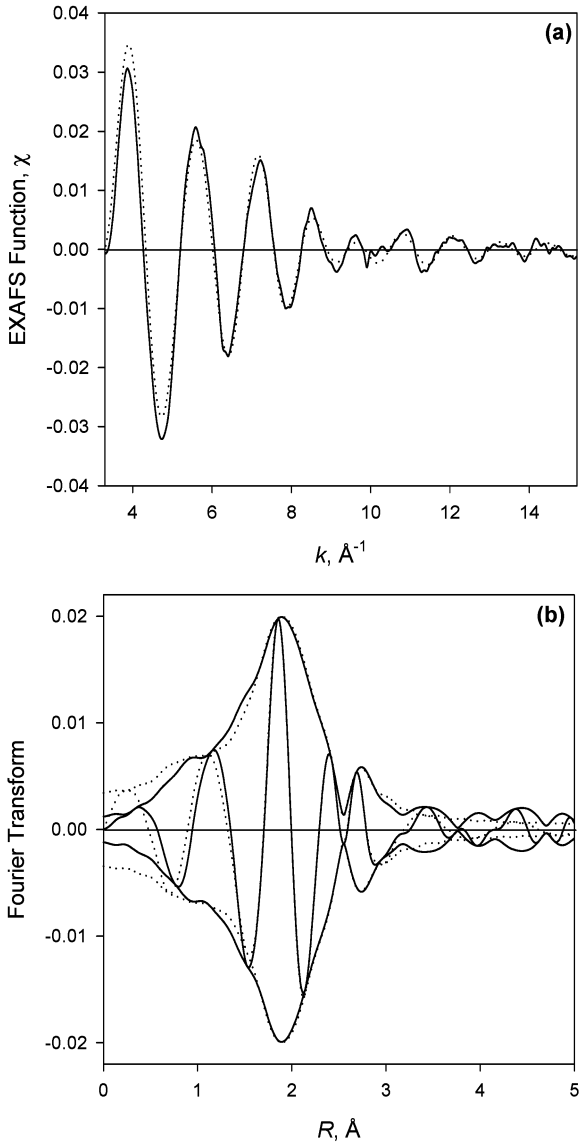

Figure 3. Results of EXAFS analysis characterizing Ir_4/NaY zeolite sample subjected to C_2H_4 flow: (a) experimental EXAFS (χ) function (solid line) and the sum of the calculated contributions (dotted line); (b) imaginary part and magnitude of uncorrected Fourier transform (k^0 weighted, $\Delta k = 3.3-15.2$ Å^{-1}) of experimental EXAFS (solid line) and sum of the calculated contributions (dotted line).

When the relatively large platinum particles on MgO and SiO_2 were investigated in similar experiments, the interactions with H_2 or hydrocarbons caused no measurable changes in the XANES region, again indicating bulklike properties of the metal in these samples.

Discussion

Comparison of Supported Metal Clusters and Particles. When supported metal particles are large enough to be bulklike, the analogies with single crystals of metal can be successfully implemented. In this case, surfaces of the crystals provide a good basis for modeling particle surfaces—as well as elucidating structures of adsorbates. Furthermore, single-crystal models can be used to obtain stoichiometries of surface reactions needed to calculate dispersions from chemisorption data. A key question about the limitations of these analogies focuses on the particle structure and size: how small can the particles become before metal−support bonding affects the metal reactivity to create new properties that are substantially different from the bulk properties of the metal? The results presented here allow some progress toward answering this question.

Effect of H_2 on Structure of γ-Al_2O_3-Supported Platinum Clusters. Hydrogen chemisorption is widely used to determine the dispersions of supported metals. The interpretations are based not only on the assumed stoichiometry of H_2 adsorption but also on the assumption that the adsorbed hydrogen does not change the structure of the supported metal. However, hydrogen should not generally be regarded as a completely innocent adsorbate, because it may induce structural (and electronic) changes in the metal, which are expected to be maximized when the clusters are smallest and the effects of the support largest; hydrogen also influences the bulk structure of some metals—and the effects are expected to be particle-size dependent. For example, hydrogen is readily taken up by bulk palladium and modifies the metal lattice, resulting in an increase of about 3% in the Pd−Pd bond distance. Such an expansion of the metal frame was detected by EXAFS spectroscopy for Al_2O_3-supported[21] and NaY zeolite-supported[22] palladium clusters of

TABLE 8: Area under the White Line Characterizing γ-Al_2O_3-Supported Platinum and Zeolite-Supported Iridium Clusters after Interaction with Various Molecules

sample	experimental conditions	area under white line, arbitrary units
Pt foil	vacuum	11.8
Pt/γ-Al_2O_3	vacuum	11.6
Pt/γ-Al_2O_3	H_2 flow	11.8
Pt/γ-Al_2O_3	partially oxidized in air at 25 °C N_2 flow	13.2
Pt/γ-Al_2O_3	completely oxidized in air at 25 °C N_2 flow	14.5
Pt/γ-Al_2O_3	C_2H_6 flow	12.0
Pt/γ-Al_2O_3	C_2H_4 flow	12.7
Pt/γ-Al_2O_3	mixture of C_2H_4 and H_2 (10:2 ratio)	12.6
Pt/γ-Al_2O_3	mixture of C_2H_4 and H_2 (1:1 ratio)	12.0
Ir_4/zeolite NaY	H_2 flow	11.2
	C_2H_4 flow	10.9
	mixture of C_2H_4 and H_2 (2:1 ratio)	10.7
	mixture of C_2H_4 and H_2 (1:1 ratio)	11.0
Ir_4/zeolite NaX	H_2 flow	11.7
	C_2H_4 flow	10.8
	mixture of C_2H_4 and H_2 (2:1 ratio)	11.8
	mixture of C_2H_4 and H_2 (1:1 ratio)	12.0

various sizes, being explained by the presence of hydrogen in the bulk metal along with chemisorbed hydrogen. Interstitial hydrogen was also found to be responsible for the disappearance of paramagnetic properties of SiO_2-supported palladium clusters 1.2 nm in average diameter.[23]

If structural changes induced by H_2 were caused solely by the presence of hydrogen in the bulk of the metal, it would be reasonable to assume that the extent of these changes would depend only on the metal's ability to absorb hydrogen. In contrast to palladium, iridium and rhodium do not absorb hydrogen substantially,[24] consistent with the unchanged structures of these metals dispersed on supports when exposed to H_2, as evidenced by EXAFS data.[25,26]

In this regard, platinum might be expected to resemble palladium more than iridium or rhodium. Thus, although platinum foil apparently does not absorb hydrogen,[27] it has been suggested[24] that platinum can take up at least some hydrogen, presumably located in subsurface regions[28,29] (this is consistent with the results of theoretical calculations[27] showing that if hydrogen would be absorbed by platinum, it would not be uniformly distributed throughout a particle, as it is in palladium).

Because the support should be regarded as a part of the ligand shell of a metal cluster on it (influencing its the electronic properties, as evidenced by XANES, atomic XAFS, and density functional theory calculations),[30−32] we suggest that adsorbed hydrogen could have effects similar to those of hydrogen in the bulk or subsurface layers. Replacement of one adsorbate by another would be expected to affect the structural changes, depending on the interactions between adsorbate and metal. There is evidence[33−35] that the Pt L_2- and Pt L_3-edge XANES of supported platinum clusters is sensitive to adsorption of hydrogen, and the electronic and geometric effects induced by chemisorbed hydrogen have evidently been isolated from each other.[33] It was concluded that hydrogen chemisorption decreases the electron density between metal atoms, leading to the relaxation of metal−metal bonds.[36] Whatever the reasons, the interactions between platinum and hydrogen are sufficient to induce changes in supported platinum similar to those observed for palladium.[21]

Our EXAFS results show that exposure of γ-Al_2O_3-supported platinum clusters to H_2 at room-temperature did not alter the platinum nuclearity, as evidenced by the unchanged Pt−Pt coordination numbers (Table 2), whereas the first-shell Pt−Pt bond distance increased by 0.06 Å relative to the value characterizing the sample after evacuation, consistent with earlier reports for platinum on various supports.[33,35] Besides the Pt−Pt distance, the metal−support interface (represented by the distance between Pt atoms in the clusters and oxygen atoms of the support) is also sensitive to the presence of hydrogen. The EXAFS data of Table 2 show that the Pt−$O_{support}$ contributions were substantially longer in the sample in the presence of H_2 (2.21 Å) than in the sample under vacuum (2.12 Å) (Table 2). A similar increase (by 0.12 Å) of the Pt−$O_{support}$ distance caused by the presence of hydrogen had been observed earlier for Pt/LTL zeolite.[11,37] These results suggest that hydrogen somehow affects the structure of the cluster-support interface. However, according to Ramaker et al.,[33] there is no substantial influence of interfacial hydrogen on the Pt−Pt distance.

There are some apparent differences illustrating that supported palladium and platinum clusters interact differently with H_2. When Pd/γ-Al_2O_3 was exposed to H_2, a 6-fold increase in the Debye−Waller factor representing the Pd−Pd contribution was observed relative to the value characterizing the sample under vacuum; this difference was explained by the presence of interstitial H_2.[21] In contrast, an increase in the relative disorder was observed when H_2 was removed from our Pt/γ-Al_2O_3 sample (Table 2) and from Pt/SiO_2,[35] consistent with the notion that the adsorbed hydrogen is part of a ligand shell, which not only changes the electronic properties of the platinum clusters but also limits the structural disorder (motion) of the Pt atoms, perhaps as a consequence of the presence of some hydrogen within the clusters. However, there are no reliable data showing how hydrogen atoms could be accommodated by small platinum clusters.

We infer that it is important that the structural changes induced by H_2 in our γ-Al_2O_3-supported platinum clusters are completely reversible. The fact that similar structural changes could not be observed when larger platinum particles were exposed to H_2 (Table 2) indicates that the interactions of H_2 with the surface of bulklike platinum alone were not sufficient to effect such changes, and we suggest that the involvement of the support is likely to be important when the changes induced by H_2 are significant.

Structural Changes Induced by Sequential Oxygen−Hydrogen Treatments. Oxygen chemisorption followed by the titration of the chemisorbed oxygen with H_2 performed at room temperature is one of the typical methods for determining platinum dispersions.[1] The chemistry is described as follows:

$$2Pt + O_2 \rightarrow 2PtO \quad (1)$$

$$PtO + {}^3/_2H_2 \rightarrow PtH + H_2O \quad (2)$$

In contrast to the interaction of platinum with H_2 described in the preceding section, the interaction of platinum with O_2 [reaction] can lead to relatively complex and drastic structural changes. The EXAFS data (Table 3) show that the stepwise exposure of completely reduced γ-Al_2O_3-supported platinum clusters to O_2 gradually decreases the Pt−Pt coordination number and bond distance (Table 3), accompanied by a gradual increase in the white line area (Table 8) and the Pt−O coordination number (from 0.3 to 2.7) and a decrease of the Pt−O distance (from 2.21 to 2.08 Å). These changes indicate a gradual oxidative fragmentation of the platinum clusters, ultimately leading to a complete loss of Pt−Pt bonds and the formation of platinum oxide species.[19]

It has been reported that oxidation at room temperature was insufficient to break all the Pt−Pt bonds in ten-atom platinum clusters in Pt/BaKLTL zeolite.[38] In contrast, it was demonstrated

that although O_2 treatment of γ-Al_2O_3-supported platinum clusters with an average diameter of about 10 Å had little effect on the Pt−Pt contributions at low temperature (−196 °C), it caused severe disruption of the Pt−Pt bonds at room temperature.[39] In agreement with this latter report, our EXAFS data show that exposure of γ-Al_2O_3-supported platinum clusters with an average diameter of approximately 11 Å to O_2 at room temperature caused complete cluster disintegration. The fact that the oxidative fragmentation could be reversed to yield platinum clusters of the same average size as those initially present implies that the oxidized species were isolated platinum oxide clusters and that no significant agglomeration had occurred.

Our EXAFS data do not allow us to distinguish between chemisorbed oxygen and oxygen associated with the support. However, the large number of O atoms in the near neighborhood of Pt atoms (the value of the total N_{Pt-O} contribution is about 3.4) is consistent with reports showing that small platinum clusters interact much more strongly with O_2 than large platinum crystallites.[40] The formation of a platinum oxide-like layer covering the platinum core is expected for larger platinum particles,[19] but the small, fully oxidized clusters on γ-Al_2O_3 may have undergone oxidation by a different mechanism.

The stepwise room-temperature titration of oxygen with hydrogen in the oxidized platinum clusters on γ-Al_2O_3 led to the reappearance of Pt−Pt contributions (Table 3) and the reconstruction of the platinum clusters. This process was accompanied by a gradual increase of the N_{Pt-Pt} and the Debye−Waller factor to values characteristic of the freshly reduced sample (Table 3), signifying that platinum was completely reconverted into clusters of the original size, at least on average. The increase of the relative disorder in the sample after contact with H_2 could be associated with a progressive increase in the number of Pt atoms present in a cluster after each stage of reduction, suggesting that larger platinum clusters exhibit a higher degree of disorder. Once again, the mechanism of the change is not evident from our data, and the water formed at room temperature during the oxidation appeared not to affect the dispersion of the resultant platinum.

Our data are consistent with reports for small clusters of other metals[38] (e.g., MgO-supported Ir_4 clusters), which could be partially or completely disrupted by exposure to O_2 at 50 or 250 °C, respectively, and re-formed almost intact by subsequent treatment in H_2 at temperatures as high as 300 °C.[41]

In summary, the data demonstrate that small supported platinum clusters interact strongly with O_2 at room temperature and undergo oxidative fragmentation, which is completely reversed when the oxidized species are treated with H_2. EXAFS spectroscopy is an efficient tool for characterizing these structural changes.

Structural Changes Caused by Interactions of Platinum Clusters with Hydrocarbons. Our EXAFS data show that the interaction of alkenes with the small γ-Al_2O_3-supported platinum clusters resulted in substantial structural changes. First, replacement of the H_2 flow by propene caused a decrease in the value of R_{Pt-Pt} from 2.76 to 2.71 Å (Table 4), which is almost the same as the R_{Pt-Pt} value observed for the sample under vacuum (Table 2). This change was reversible, as the subsequent replacement of the propene flow with H_2 reversed the R_{Pt-Pt} value back to 2.76 Å (Table 4). Exposure of this sample to ethene had a similar effect on R_{Pt-Pt}, and the changes were once again found to be reversible (Table 4).

Observed changes in R_{Pt-Pt} may be evidence of the role of the initially present hydrogen on the metal. Microcalorimetric data[42] indicate that H_2 adsorbs dissociatively on clean platinum with an initial heat of adsorption of about 90 kJ/mol; the initial heat of adsorption of alkenes is about 160 kJ/mol, consistent with the inference that alkenes interact more strongly with platinum than hydrogen. Therefore, upon exposure of the sample to alkene, the hydrogen chemisorbed on the platinum clusters might simply have been displaced, as was demonstrated for platinum powder;[42] alternatively, the hydrogen could be consumed in an alkene hydrogenation reaction. Whatever the nature of the process, it resulted in changes in the distance R_{Pt-Pt} similar to those detected upon evacuation and subsequent exposure of the γ-Al_2O_3-supported platinum clusters to H_2 (Table 2).

In contrast, when H_2 was replaced by ethane, the value of R_{Pt-Pt} remained almost unchanged (Table 4), consistent with the suggestion that ethane did not replace the adsorbed hydrogen. Under some conditions, ethane reacts with clean platinum surfaces, undergoing extensive dehydrogenation and resulting in the formation of Pt−H bonds.[43] There is no evidence of such chemistry in our experiments.

The greatest changes in the value of N_{Pt-Pt} were observed when completely reduced Pt/γ-Al_2O_3 was exposed to flowing alkenes (Table 4). The samples became more disordered, as evidenced by the increased Debye−Waller factors. These changes were reversible, including the changes in the metal−support interface, as indicated by the $N_{Pt-O_{support}}$ and $R_{Pt-O_{support}}$ values (Table 4). We infer that it is important that the electronic structure of the platinum clusters also changed, as evidenced by the changed area under the white line (Table 8). Thus, the data are consistent with modification of both electronic and structural properties of platinum clusters exposed to alkenes. We infer that the changes observed in the metal−support interface together with those characterizing the Pt−Pt contributions are indicative of morphological transformations of the platinum clusters, such as flattening, for example, resulting in a larger number of bonds between Pt atoms and O atoms of the support, characterized by the EXAFS contributions at the shorter $Pt-O_s$ distance (Table 4). These structural changes were more pronounced in the case of ethene than propene.

The changes resulting from interactions of the hydrocarbons with the supported platinum are consistent with what is known about how alkanes and alkenes interact with platinum. Calorimetric data indicate that the initial heats of adsorption of alkanes on clean platinum surfaces are about 240−280 kJ/mol, much greater than those characterizing adsorption of alkenes (146−178 kJ/mol).[43] Such high initial heats of adsorption were interpreted as evidence of cracking and partial dehydrogenation of the alkanes upon adsorption, resulting in the formation of Pt−H and Pt−C bonds.[43] These reactions are site-demanding and usually terminated when the appropriate sites are filled. In contrast, the chemisorption of alkenes takes place without fragmentation and is less site-demanding, as illustrated by the ability of ethene to interact with platinum surfaces already saturated by ethane.[43] Low-energy electron diffraction (LEED) and sum frequency generation data show that π-bonded ethene, di-σ-bonded ethene, and ethylidyne formed when ethene was brought in contact with platinum.[44−48] According to quantum mechanical calculations, the heats of ethene adsorption on platinum clusters to form the π-bonded, di-σ-bonded ethane, or ethylidyne species are 95, 135, and 155 kJ/mol, respectively,[49] demonstrating that the ethylidyne has the strongest bonds to the surface. π-Bonded ethene is the least stable of these species and could be identified best at temperatures below −78 °C.[50] Di-σ-bonded ethene is more strongly bound than π-bonded ethene and could be observed even under vacuum.[51] However, ethylidyne dominates on platinum at room temperature, being

formed by the dissociative adsorption of ethene, resulting in the loss of one hydrogen atom per ethene molecule and repositioning of molecules so that the C−C axis becomes perpendicular to the metal surface.[42] Hydrogen atoms released during this process and located on the surface may interact with ethene to form ethane.[42] The ethylidyne bonds to three Pt atoms in 3-fold fcc sites.[47,51,52]

Scanning tunneling microscopy data[53] and theoretical calculations[52] illustrate that ethylidyne is mobile on the metal surface at room temperature, moving between 3-fold fcc and hcp sites. Being strongly bonded to the surface, the ethylidyne species are known for restructuring of Pt(111) and Rh(111), as demonstrated by LEED data[54] and confirmed by calculations at the density functional level.[55]

In our analysis of EXAFS data, we did not consider it realistic to try to identify Pt−C contributions in samples exposed to alkenes, because of difficulties in separating these contributions from the $Pt-O_{support}$ contributions that were characterized by large Debye−Waller factors. However, we suggest that the formation of ethylidyne-like species from ethene on the γ-Al_2O_3-supported platinum clusters could be a driving force for the observed structural changes. Being strongly bonded to 3-fold Pt sites, such species would be part of the ligand shells of platinum clusters, and the morphological changes could be regarded as a modification of the clusters to minimize their energy.

This suggestion is reinforced by the EXAFS data (Table 4) illustrating that when platinum clusters were exposed to ethane, N_{Pt-Pt} was only slightly changed relative to changes observed after the exposure to alkenes. Moreover, the exposure to ethane had a minimal effect on the electronic structure of platinum, as evidenced by the relatively small change of the white line area (Table 8). Realizing that observed changes were small (and even possibly negligible), we nonetheless suggest that they may be indicative of structural rearrangements of platinum clusters caused by their weak interactions with alkanes. We infer that the different adsorption properties of alkanes and alkenes reflected in the different nature of the surface species formed on platinum that require different surface sites, which may be related to cluster size, but we lack sufficient information to explain these issues or the different interactions of ethene and propene with platinum clusters.

Interaction of Platinum Particles with Hydrocarbons. Being highly dispersed with nearly all the Pt atoms exposed, the platinum clusters with an average diameter of approximately 11 Å were characterized by first-shell Pt−Pt contributions and no higher-shell Pt−Pt contributions. Larger platinum particles, such as those formed on MgO or SiO_2 have higher-shell Pt−Pt contributions (Table 2). Characterization of such samples only in terms of the changes in the first-shell Pt−Pt contributions is insufficient and could lead to misinterpretation of data. For example, the EXAFS data show that the values of N_{Pt-Pt} characterizing the first-shell Pt−Pt contributions of the particles that were 21 Å in average diameter on MgO were not changed when the sample was exposed to the ethene or propene compared to those observed for the sample under H_2 flow (Table 5).

These observations do not mean that platinum particles of such sizes are completely resistant to structural changes. Realizing that only exposed metal atoms were involved in interactions with hydrocarbons, we infer (on the basis of a simple geometry) that the higher metal−metal shells in the EXAFS data are expected to provide the most accurate representation of the surface atoms. The choice of the most appropriate shell for inferring structural changes in particles appears to depend on the number of atoms in the particle. For example, analysis of the second and third coordination shells representing the MgO-supported platinum particles (21 Å in average diameter) was sufficient to demonstrate changes induced by the interactions with hydrocarbons. Our EXAFS data (Table 5) show that values of N_{Pt-Pt} characterizing the second- and third-shell Pt−Pt contributions in the spectra of Pt/MgO decreased substantially when the sample was exposed to ethene or propene, with the effect being greater for ethene. These changes, together with the data showing an increase in the $N_{Pt-O_{support}}$ contributions (Table 5), are indicative of changes in platinum morphology.

In general, the changes observed for the MgO-supported platinum particles exhibit the same trends and direction as those observed for the much smaller γ-Al_2O_3-supported platinum clusters (Table 4). We emphasize that these changes in the particles on MgO are much smaller than those observed for the smaller clusters on γ-Al_2O_3.

In summary, this comparison provides the basis for a generalization of the influence of hydrocarbons on the structure of supported platinum: When the platinum particles were large enough (such as those on SiO_2, 45 Å in average diameter), no changes were observed in values characterizing the first-, second-, or third-shell Pt−Pt contributions (Table 5). Increasingly larger changes were observed for decreasing particle/cluster sizes. The lack of evident changes in the EXAFS parameters for the largest particles does not reflect a lack of structural changes in these particles; rather, the data characterizing the three Pt−Pt shells are not sensitive to changes in the surface layers of Pt atoms. The separation and analysis of higher shells is beyond our present capabilities with EXAFS spectroscopy.

Structural Changes Observed Under Conditions of Alkene Hydrogenation Catalysis. Platinum is a highly active catalyst for hydrogenation of alkenes, with the reaction proceeding rapidly even at room temperature. Ethene hydrogenation, for example, has been inferred to proceed on platinum surfaces via the dissociative adsorption of H_2 and ethene, giving surfaces that typically incorporate ethylidyne and atomic hydrogen;[51] migration of ethylidyne between fcc and hcp 3-fold sites opens up positions for adsorption of π-bonded ethene. The concentration of π-bonded species on platinum is typically only about 4% of a monolayer, but the stepwise hydrogenation of these species accounts for most of the ethane formed.[51] Thus, ethylidyne could be regarded as a spectator on platinum during catalysis, and the molecularly adsorbed ethene is believed to be the reactive species. Although barely reactive, ethylidyne may impose morphological changes on supported platinum clusters, as suggested by our EXAFS data.

Assuming that ethylidyne is responsible for reconstruction of platinum, one might suggest that the morphology of platinum clusters under reaction conditions will depend on the presence or absence of such species. The occurrence of ethylidyne on platinum surfaces depends on the composition of the reactant. For example, it was shown by IR spectroscopy that during ethene hydrogenation at room temperature on Pt/SiO_2, ethylidyne was not detected in the presence of H_2-rich mixtures but was detected when the reaction mixture was deficient in H_2.[56] These results provide a basis for understanding the structural changes observed by EXAFS during our monitoring of alkene hydrogenation catalyzed by Pt/γ-Al_2O_3 (Table 6).

Significant changes in the EXAFS data representing Pt/γ-Al_2O_3 (Table 6) were observed only when the amount of H_2 in the reaction feed was not enough to completely hydrogenate

the alkene (propene/H_2 = 2:1 or ethene/H_2 = 5:1), consistent with high concentrations of alkenes in the gas phase in contact with the catalyst under reaction conditions. It was suggested that at low coverages ethene is bonded to platinum with the C−C axis parallel to the surface plane; however, at high coverages the species with the C−C axis perpendicular to the metal surface prevails.[43] Thus, under our conditions, the surface of platinum in Pt/γ-Al_2O_3 would be expected to have a substantial coverage of strongly bonded ethylidyne, as was observed for Pt/SiO_2.[56] Indeed, we found that the values of N_{Pt-Pt} and R_{Pt-Pt} in this case are much smaller than those observed when the sample was exposed to H_2 (Table 6), consistent with the inference that the structure of the platinum clusters was changed under these conditions. However, the fact that the N_{Pt-Pt} and R_{Pt-Pt} values were exactly the same as those of the sample exposed to pure alkenes (Table 4) leads us to suggest that the platinum structures in these two cases were similar or even almost identical. This suggestion is reinforced by the XANES data (Table 8) showing that exposure of the sample to pure ethene has nearly the same effect on the electronic properties of platinum as the exposure to the ethene-hydrogen mixture enriched in ethene.

The situation was easily reversed by addition of more H_2 to the feed to the reactor. The EXAFS data indicate only a small change in the N_{Pt-Pt} values when the concentration of H_2 in the feed became high enough to completely hydrogenate the ethene (Table 6). Only ethane was detected in the gas phase in contact with the catalyst under these conditions, and the formation of ethylidyne is not expected to have occurred with this feed composition.[42,56] Correspondingly, the EXAFS and XANES data (Tables 6 and 8) show that the electronic and structural properties of platinum clusters remained largely unchanged when the sample was in contact with alkanes.

Thus, the EXAFS data of Table 6 demonstrate dynamic morphological changes of the relatively small γ-Al_2O_3-supported platinum clusters that correspond to changes of the reaction feed composition. Being reversible, such changes demonstrate that the surfaces (and morphologies) of these clusters are sensitive to the reaction environment and constantly adjust under the reaction conditions, presumably to satisfy demands induced by various reactants and products that act as ligands. The data are also consistent with the inference that the presence on the platinum of strongly bonded ligands, such as ethylidyne, for example, is a primary reason for the observed morphological changes and electron-deficiency of platinum.

This suggestion is reinforced by the EXAFS data reported for Pt/LTL zeolite and illustrates the reconstruction of the platinum into small clusters incorporating approximately three metal atoms each on average when the sample was exposed to CO.[57] Similarly, γ-Al_2O_3-supported platinum particles with an average diameter of about 27 Å were restructured to give isolated oxidized platinum species as a result of interaction with NO.[58] In contrast, the morphology of platinum was essentially unchanged under conditions of *n*-hexane isomerization, as evidenced by EXAFS data.[59] Because the sample was expected to be in contact only with various alkanes during this reaction, these data are consistent with our observations.

Lack of Structural Changes of Extremely Small Metal Clusters. The data discussed above provide insights illustrating how platinum clusters with an average diameter of about 11 Å or larger may interact with various reactants. It remains largely unknown, however, what would happen when smaller platinum clusters are exposed to the reaction mixtures. Because it is not known how to prepare well-defined platinum clusters incorporating only a few Pt atoms on a porous metal oxide support, even when organometalllic precursors are used (in part because of the high mobility of Pt atoms and their tendency to aggregate),[60] we turned to iridium clusters instead; these can be prepared from iridium carbonyls precursors (such as $Ir_4(CO)_{12}$) to incorporate only a few (such as four) Ir atoms.[61]

The EXAFS data of Table 7 show that the structural parameters characterizing zeolite NaY- or zeolite NaX-encaged iridium clusters approximated as Ir_4 remained almost unchanged from those representing the same sample under H_2, when the clusters were exposed to ethene or mixtures of ethene and H_2 of various compositions. The data are consistent with earlier reports indicating that the reaction environment has almost no effect on the framework structure of iridium or rhodium clusters modeled as Ir_4, Ir_6, or Rh_6.[25,26,62−64]

The lack of structural changes may indicate significant differences between platinum and iridium, but we suggest that it is more likely that the smallness of the metal clusters plays a more significant role than the nature of the metal. MgO- and γ-Al_2O_3-supported four- or six-atom clusters of iridium and of rhodium are active for the hydrogenation of alkenes.[62−64] Moreover, alkene hydrogenation catalyzed by such small clusters appears to be similar to that on extended metal surfaces in terms of the reaction kinetics and mechanism.[63] Assuming that the mechanism of alkene hydrogenation was essentially the same on iridium and platinum clusters, we suggest that the reactions of alkenes with iridium clusters generate surface species similar to those observed on platinum (as referred to above).

Indeed, ethyl, di-σ-bonded ethene, and π-bonded ethene were identified by IR spectroscopy on supported Ir_4 and Ir_6 under catalytic reaction conditions.[62−64] As for supported platinum, ethylidyne was observed on Ir_4 supported on γ-Al_2O_3 under reaction conditions, but only in ethene-rich mixtures.[62] In contrast, propylidyne was detected on Ir_4/γ-Al_2O_3 during propene hydrogenation, even in excess H_2, but it was not observed when the support was MgO, indicating a possible influence of the support.[63] Considering the support as a ligand, it is reasonable to assume that the strongest ligand effects exerted by supports would be expected for the smallest supported metal clusters and negligible for large supported metal particles with only a small fraction of the metal atoms located at the metal−support interface.[64] It is also expected that the MgO and γ-Al_2O_3 supports would have different effects as ligands on the small iridium clusters because of differences in their electron-donor properties. MgO, a strong base, would favor the increase of the charge density on Ir_4 compared to that on γ-Al_2O_3 and consequently influence the strength of hydrocarbon−iridium interactions in hydrogenation catalysis, thereby influencing the catalytic activity.[64]

In contrast to these ligand effects,when ethylidyne forms on the Ir_4 clusters, there is a sufficient number of metal atoms to accommodate only one ethylidyne molecule per cluster. Clusters with fewer than three metal atoms would not be able to accommodate such species at all, as illustrated by data reported for the mononuclear Re complexes bonded to highly dealuminated Y zeolite indicating other hydrocarbons but not ethylidyne.[65]

The picture does not require any structural changes in Ir_4 clusters for catalysis to occur, consistent with the experimental observations. It is likely that metal clusters as small as Ir_4 (or perhaps three-atom clusters) represent a (near) limiting case because of the number of metal atoms involved. Being structurally ideal for the adsorption of ethylidyne or similar species that are not reactive intermediates, the Ir_4 clusters have only a

limited number of remaining sites to accommodate reactive intermediates such as π- or di-σ-bonded alkenes. The strong adsorption of ethylidyne-like species on Ir_4 would require three of the four metal atoms to accommodate them (and it is not clear to what extent the Ir atoms bonded to the support play a role in catalysis). The existence of only one available metal atom may be sufficient for alkene hydrogenation to proceed, as mononuclear metal complexes (such as Wilkinson's complex), including oxide-supported complexes, are active for alkene hydrogenation.[65] The mobility of ethylidyne on such small iridium clusters is expected to be low because of the isolation of the clusters from each other on the support and the limited number of adsorption sites. Thus, it is possible that clusters incorporating a few metal atoms with alkylidyne ligands are inactive for alkene hydrogenation and only the clusters lacking these ligands are active. The possible inhibition by such species may account in part for the relatively low activities of clusters as small as Ir_4 relative to larger clusters for alkene hydrogenation.[66]

The possible contribution of the support to the relatively high structural stability of the iridium clusters under reaction conditions is not entirely understood. It was suggested to be related to the polarization of the clusters and the formation of ionic bonds between oxygen anions of the support and metal atoms present as cations in the clusters at the metal−support interface.[2] This interpretation might help to explain the reduced interactions with hydrogen of small metal clusters on zeolites having a large negative framework charge.[67] The question of how much the presence of other adsorbates (such as alkenes and alkanes) could be altered by such effects also remains open.

Conclusions

Platinum clusters of various sizes, ranging from 11 to 45 Å in average diameter, were formed on γ-Al_2O_3, MgO, and SiO_2 from $PtCl_2(PhCN)_2$ after reduction with H_2 at 400 °C. The surface species were characterized by EXAFS spectroscopy before and after exposure to H_2, O_2, alkenes, and alkanes, as well as during alkene hydrogenation catalysis at room temperature. The data demonstrate that the effects of adsorbates on the structure of the larger platinum clusters (21 Å) formed on MgO and platinum particles (45 Å) formed on SiO_2 were much smaller than on the highly dispersed platinum clusters (11 Å) formed on γ-Al_2O_3.

Exposure of Pt/γ-Al_2O_3 to H_2 did not change the morphology of the platinum clusters, as the Pt−Pt first-shell coordination number remained unchanged. However, it did lead to an increase in the Pt−Pt bond distance and a decreased in the Debye−Waller factor. In contrast, exposure of the sample to O_2 led to the fragmentation of the platinum clusters and formation of site-isolated platinum oxide clusters. Subsequent treatment of the sample with H_2 led to restoration of platinum clusters of the same average size as those present initially, as evidenced by reappearance of identical Pt−Pt contributions in the EXAFS spectra.

The interaction of alkenes and alkanes with γ-Al_2O_3-supported platinum clusters did not influence the Pt−Pt bond distance. However, when the sample was exposed to alkenes, the first-shell Pt−Pt coordination number decreased, consistent with changes in morphology of the platinum clusters. These were accompanied by an increase of the white line area, suggesting that the interaction of hydrocarbons with platinum clusters led to withdrawal of electron density from platinum with the effect maximized for alkenes. The observed changes were reversible, and the sample could easily be returned to the original state by the interaction with H_2.

The EXAFS data demonstrate that under conditions of alkene hydrogenation catalysis, which proceeds at high rates on γ-Al_2O_3-supported platinum clusters even at room temperature, the electronic properties and the structure of platinum clusters depend on the reactant composition and the nature of the molecules involved in the reaction process.

In contrast to the supported platinum clusters, the zeolite-supported Ir_4 clusters are characterized by a lack of changes in the structure of the metal frame resulting from exposure to H_2, alkenes, or mixtures of the two. The contrast is explained (at least in part) by differences in the nature of the metals and the small size of the iridium clusters, which represents a near limiting case because the number of metal atoms limits what can bond to them.

Acknowledgment. We thank M. Boudart for many stimulating discussions. This research was supported by the U.S. Department of Energy, Office of Basic Energy Sciences (FG02-87ER13790 and FG02-04ER15513 for F.L. and B.C.G. and DE-FG02-96ER14666 for O.S.A. and M.D.A.) and the National Science Foundation (CTS-9615257). We acknowledge the NSLS, which is supported by the U.S. Department of Energy, and the staffs of beamlines X-18B and X-11A.

References and Notes

(1) Boudart, M.; Djéga-Mariadassou, G. *Kinetics of Heterogeneous Catalytic Reactions*; Princeton University Press: Princeton, NJ, 1984.
(2) Vayssilov, G. N.; Gates, B. C.; Rösch, N. *Angew. Chem., Int. Ed.* **2003**, *42*, 1391.
(3) Topsøe, H. *Stud. Surf. Sci. Catal.* **2000**, *130*, 1.
(4) Alexeev, O.; Gates, B. C. *Stud. Surf. Sci. Catal.* **2000**, *130*, 371.
(5) Ichikawa, M. In *Metal Clusters in Chemistry*; Braunstein, P., Oro, L. A., Raithby, P. R., Eds.; Wiley-VCH: Weinheim, 1999; p 1273.
(6) Kawi, S.; Chang, J.-R.; Gates, B. C. *J. Phys. Chem.* **1993**, *97*, 10599.
(7) Kawi, S.; Gates, B. C. *J. Phys. Chem.* **1995**, *99*, 8824.
(8) Kawi, S.; Gates, B. C. *Catal. Lett.* **1991**, *10*, 263.
(9) Beutel, T.; Kawi, S.; Purnell, S. K.; Knözinger, H.; Gates, B. C. *J. Phys. Chem.* **1993**, *97*, 7284.
(10) Odzak, J. F.; Argo, A. M.; Lai, F. S.; Gates, B. C.; Pandya, K.; Feraria, L. *Rev. Sci. Instrum.* **2001**, *72*, 3943.
(11) Alexeev, O.; Panjabi, G.; Gates, B. C. *J. Catal.* **1998**, *173*, 196.
(12) Vaarkamp, M.; Linders, J. C.; Koningsberger, D. C. *Physica B* **1995**, *208−209*, 159.
(13) Koningsberger, D. C. In *Synchrotron Techniques in Interfacial Electrochemistry*; Melendres, C. A., Tadjeddine, A., Eds.; Kluwer: Dordrecht, 1994; p 181.
(14) Stern, E. A. *Phys. Rev. B* **1993**, *48*, 9825.
(15) Brigham, E. O. *The Fast Fourier Transform*; Prentice Hall: Englewood Cliffs, NJ, 1974.
(16) Kirlin, P. S.; van Zon, F. B. M.; Koningsberger, D. C.; Gates, B. C. *J. Phys. Chem.* **1990**, *94*, 8439.
(17) van Zon, J. B. A. D.; Koningsberger, D. C.; van't Blik, H. F. J.; Sayers, D. E. *J. Chem. Phys.* **1985**, *82*, 5742.
(18) Kip, B. J.; Duivenvoorden, F. B. M.; Koningsberger, D. C.; Prins, R. *J. Catal.* **1987**, *105*, 26.
(19) Weber, R. S.; Boudart, M.; Gallezot, P. In *Growth and Properties of Metal Clusters*; Bourdon J., Ed.; Elsevier: Amsterdam, 1980; p. 415.
(20) Bzowski, A.; Sham, T. K.; Yiu, Y. M. *Phys. Rev. B* **1994**, *49*, 13776.
(21) Davis, R. J.; Landry, S. M.; Horsley, J. A.; Boudart, M. *Phys. Rev. B* **1989**, *39*, 10580.
(22) Moraweck, B.; Clugnet, G.; Renouprez, A. *J. Chim. Phys.* **1986**, *83*, 265.
(23) Ladas, S.; Dalla Betta, R. A.; Boudart, M. *J. Catal.* **1978**, *53*, 356.
(24) Wagner, F. E.; Wortmann, G. In *Hydrogen in Metals. 1. Basic Properties*; Alefeld, G., Voelkl, J., Eds.; Springer-Verlag: Berlin, 1978; p 131.
(25) Panjabi, G.; Argo, A. M.; Gates, B. C. *Chem. Eur. J.* **1999**, *5*, 2417.
(26) Weber, W. A.; Zhao, A.; Gates, B. C. *J. Catal.* **1999**, *182*, 13.
(27) Ohtani, K.; Fujikawa, T.; Kubota, T.; Asakura, K. *Jpn. J. Appl. Phys.* **1997**, *36*, 6504.
(28) Paalo, Z., Menon, P. G. *Hydrogen Effects in Catalysis*; Marcel Dekker: New York, 1988.
(29) Ichikuni, N.; Iwasawa, Y. *Catal. Lett.* **1993**, *20*, 87.
(30) Ramaker, D. E.; de Graaf, J.; van Veen, J. A. R.; Koningsberger, D. C. *J. Catal.* **2001**, *203*, 7.

(31) Mojet, B. L.; Miller, J. T.; Ramaker, D. E.; Koningsberger, D. C. *J. Catal.* **1999**, *186*, 373.
(32) Koningsberger, D. C.; Oudenhuijzen, M. K.; de Graaf, J.; van Bokhoven, J. A.; Ramaker, D. E. *J. Catal.* **2003**, *216*, 178.
(33) Ramaker, D. E.; Mojet, B. L.; Garriga Oostenbrink, M. T.; Miller, J. T.; Koningsberger, D. C. *Phys. Chem. Chem. Phys.* **1999**, *1*, 2293.
(34) Kubota, T.; Asakura, K.; Ichikuni, N.; Iwasawa, Y. *Chem. Phys. Lett.* **1996**, *256*, 445.
(35) Reifsnyder, S. N.; Otten, M. M.; Sayers, D. E.; Lamb, H. H. *J. Phys. Chem. B* **1997**, *101*, 4972.
(36) Sanchez, M. E.; Jansen, A. P. J.; van Santen, R. A. *Chem. Phys. Lett.* **1990**, *167*, 399.
(37) Vaarkamp, M.; Mojet, B. L.; Kappers, M.; Miller, J. T.; Koningsberger, D. C. *J. Phys. Chem.* **1995**, *99*, 16067.
(38) Deutsch, S. E.; Miller, J. T.; Tomishige, K.; Iwasawa, Y.; Weber, W. A.; Gates, B. C. *J. Phys. Chem.* **1996**, *100*, 13408.
(39) Fukushima, T.; Katzer, J. R.; Sayers, D. E.; Cook. J. In *Proceedings of the 7th International Congress on Catalysis*; Seiyama, T. Tanabe, K., Eds.; Elsevier: Amsterdam, 1981; p 79.
(40) Jaeger, N. I.; Jourdan, A. L.; Schulz-Ekloff, G. *J. Chem. Soc., Faraday Trans.* **1991**, *87*, 1251.
(41) Lai, F. S.; Gates, B. C. *Nano Lett.* **2001**, *1*, 583.
(42) Spiewak, B. E.; Cortright, R. D.; Dumesic, J. A. *J. Catal.* **1998**, *176*, 405.
(43) Pálfi, S.; Lisowski, W.; Smutek, M.; Ćerny, S. *J. Catal.* **1984**, *88*, 300.
(44) Cremer, P. S.; Su, X. C., Shen; Y. R., Somorjai, G. A. *J. Am. Chem. Soc.* **1996**, *118*, 2942.
(45) Doll, R.; Gerken, C. A.; Van Hove, M. A.; Somorjai, G. A. *Surf. Sci.* **1997**, *374*, 151.
(46) Cremer, P.; Stunners, C.; Niemantsverdriet, J. W.; Shen, Y. R.; Somorjai, G. A. *Surf. Sci.* **1995**, *328*, 111.
(47) Starke, U.; Barbieri, A.; Materer, N.; Van Hove, M. A.; Somorjai, G. A. *Surf. Sci.* **1993**, *286*, 1.
(48) Wander, A.; Van Hove, M. A.; Somorjai, G. A. *Phys. Rev. Lett.* **1991**, *67*, 626.
(49) Watwe, R. M.; Spiewak, B. E.; Cortright, R. D.; Dumesic, J. A. *J. Catal.* **1998**, *180*, 184.
(50) Cassuto, A.; Kiss, J.; White, J. M. *Surf. Sci.* **1991**, *255*, 289.
(51) Hwang, K. S.; Yang, M.; Zhu, J.; Grunes, J.; Somorjai, G. A. *J. Mol. Catal. A: Chem.* **2003**, *204*, 499.
(52) Nomikou, Z.; Van Hove, M. A.; Somorjai, G. A. *Langmuir* **1996**, *12*, 1251.
(53) Land, T. A.; Michely, T.; Behm, R. J.; Hemminger, J. C.; Comsa, G. *J. Chem. Phys.* **1992**, *97*, 6774.
(54) Van Hove, M. A.; Somorjai, G. A. *J. Mol. Catal. A: Chem.* **1998**, *131*, 243.
(55) Ge, Q.; King, D. A. *J. Chem. Phys.* **1999**, *110*, 4699.
(56) Rekoske, J. E.; Cortright, R. D.; Goddard, S. A.; Sharma, S. B.; Dumesic, J. A. *J. Phys. Chem.* **1992**, *96*, 1880.
(57) Mojet, B. L.; Miller, J. T.; Koningsberger, D. C. *J. Phys. Chem. B* **1999**, *103*, 2724.
(58) Asakura, K.; Chun, W.-J.; Shirai, M.; Tomishige, K.; Iwasawa, Y. *J. Phys. Chem. B* **1997**, *101*, 5549.
(59) Otten, M.; Clayton, M. J.; Lamb, H. H. *J. Catal.* **1994**, *149*, 211.
(60) Purnell, S. K.; Sanchez, K. M.; Patrini, R.; Chang, J. R.; Gates, B. C. *J. Phys. Chem.* **1994**, *98*, 1205.
(61) Gates, B. C. *J. Mol. Catal. A: Chem.* **2000**, *163*, 55.
(62) Argo, A. M.; Odzak, J. F.; Gates, B. C. *J. Am. Chem. Soc.* **2003**, *125*, 7107.
(63) Argo, A. M.; Gates, B. C. *Langmuir* **2002**, *18*, 2152.
(64) Argo, A. M.; Odzak, J. F.; Gates, B. C. *Nature (London)* **2002**, *415*, 623.
(65) Enderle, B.; Gates, B. C. *J. Mol. Catal. A: Chem.* **2003**, *204*−*205*, 473.
(66) Xu, Z.; Xiao, F.-S.; Purnell, S. K.; Alexeev, O.; Kawi, S.; Deutsch, S. E.; Gates, B. C. *Nature (London)* **1994**, *372*, 346.
(67) Xu, L.; Zhang, Z.; Sachtler, W. M. H. *J. Chem. Soc., Faraday Trans.* **1992**, *88*, 2291.